Tsukuba Geoenvironmental Sciences, Vol. 9, pp. 13-19, Dec. 26, 2013

Time-lapse photography applied to monitoring of alpine slope processes

Norikazu MATSUOKA*

Abstract

Interval cameras visually monitored soil movements and rockfalls in a periglacial zone of the southern Japanese Alps. The time-series images greatly improve understanding of slope processes in remote, seasonally inaccessible areas. They detect the timing of slope movements at a high temporal resolution. They visualize both slow progressive movements (frost creep) and rapid temporary movements (rill erosion and rockfalls). Stereographic view of successive images displays 3D slope movements that indicate the location and magnitude of displacement. When combined with sensor-based data logging, visual monitoring allows more reliable evaluation of thresholds (environmental controls) for slope movements.

Key words: time-lapse photography, slope processes, frost creep, rockfall, Japanese Alps

I. Introduction

Monitoring of slope processes is essential in quantitative evaluation of mountain landscapes and prediction of natural hazards induced by mass movements. During the last three decades sensor-based ('blind') data logging has become popular in a wide range of geomorphological research and has promoted acquisition of data on slow and rapid mass movements and their environmental controls. Sensor-based monitoring is particularly useful in remote areas like high mountains, deserts and polar regions where accessibility and electricity are extremely limited (e.g. Matsuoka, 2006; Harris et al., 2011; Girard et al., 2013). However, the reliability of data is sometimes questionable and the interpretation is often equivocal. To improve the reliability and interpretation requires 'visual' information on the monitoring site.

Time-lapse photography (interval cameras) has recently been launched onto field studies to record visual images of the targets at certain intervals. Some models operate year-round even under cold climate without manual maintenance. The camera images allow us to confirm the movements and/or environmental conditions indicated by sensor-based monitoring, as well as to extend point information provided by sensors to areal information (e.g. Christiansen, 2005; Barchyn and Hugenholtz, 2012; Scambos et al., 2013). This paper presents examples of time-lapse photography applied to monitoring of rock and soil movements in the southern Japanese Alps and demonstrates how visual information improves the interpretation of slope processes. The monitoring sites on southern slopes of Mt. Ainodake (3189 m ASL) are situated in a periglacial zone above the tree line. The slopes lack permafrost but experience deep seasonal frost (Matsuoka, 1998; Matsuoka and Sakai, 1999).

2. Instrumentation

Two types of interval cameras were used: KADEC-EYE II (acronym: KE) manufactured by North One (Japan) and TimelapseCam 8.0 (acronym: TLC) manufacture by Wingscapes (USA). KE operates with a sealed lead-acid battery (DC 6 V, 3.0–4.5 Ah) and records images in a Compact Flash disk with a resolution of 1.3 M pixel (one shot requires 130 KB). In addition to shooting at regular intervals up to 24 h, KE can suspend operation during the night. TLC operates with four AA batteries (in total DC 6V with a series circuit) and records images in an SD card with a resolution of 0.3–8.0 M pixel (one shot consumes 180 KB to 2 MB) at regular intervals up to 24 h. Both cameras operate year-round without replacement of battery when recording at daily intervals. These interval cameras targeted two kinds of mass movements: soil movements (frost creep) on a stone-banked lobe and rockfalls from a rockslide cliff.

The interval cameras were mounted on a four-leg pole anchored in large stable stones and faced the targets. Strong winds and blizzards during the winter (~30 m/s), however, occasionally caused rotation or toppling of the pole, which interrupted recording of the targets. Images were also unavailable or obscured when fog or rain masked the targets. On occasion mechanical troubles happened. A KE camera went out of control and consumed the battery quickly. A TLC camera recorded red-filtered images during most of the winter months due to an unknown reason; but the images are still visible despite the lowered quality. Otherwise, continuous images were obtained.

Multisensor data logging was concurrently undertaken to monitor factors controlling the slope movements: soil temperature and moisture at different depths, as well as vertical soil movement (frost heave) for frost creep; rock temperature at different depths and rock-joint opening for rockfalls; and meteorological conditions including air temperature, humidity, wind speed and direction, precipitation and air pressure for both processes. The details of

* Faculty of Life and Environmental Sciences, University of Tsukuba

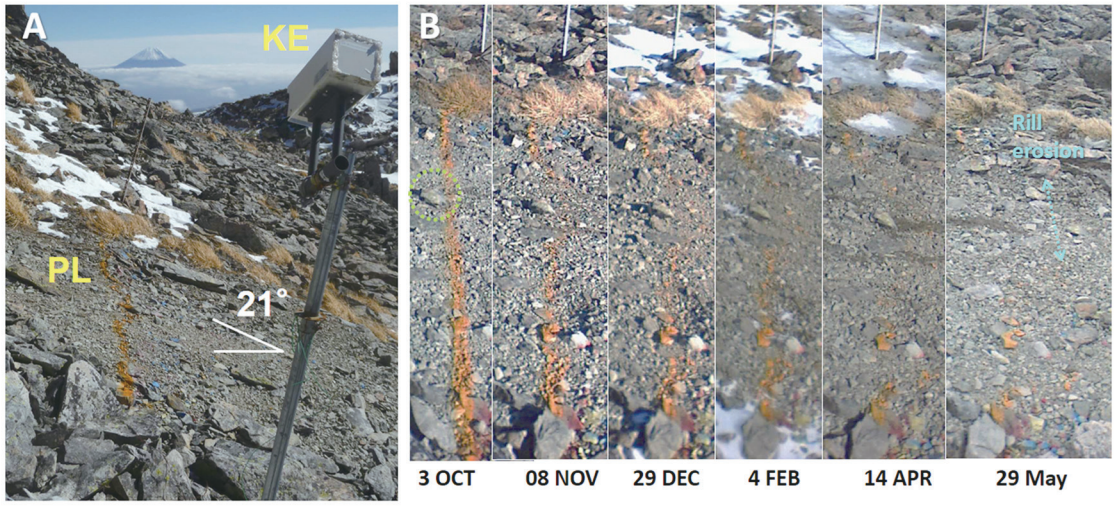

Fig. 1. Monitoring soil movements on a stone-banked lobe in the 2009–2010 period.(A) Instrumentation. KE = KADEC-EYE II camera, PL = painted line (orange).(B) Time series of soil movements indicated by a painted line. Note the location of a stone (dotted circle) that progressively displaced downslope until 14 April and disappeared by 29 May.

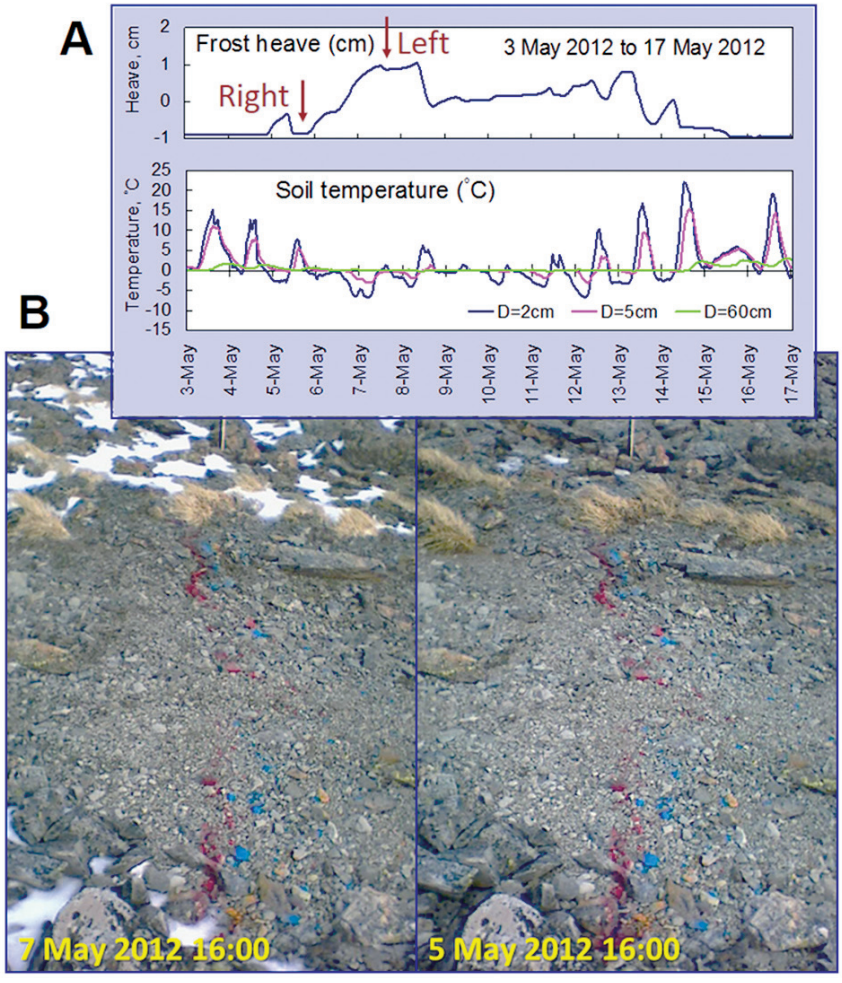

Fig. 2. Stereographic view of a frost heave event in May 2012. (A) Vertical soil movement recorded with an extensometer (located upslope of the painted line) and soil temperatures at different depths during the event (heave amount 2 cm). Arrows indicate the timings of shots in B. (B) A stereoscopic pair of images taken before and after a frost heave event. The stereogram indicates three-dimensional frost heaving, the magnitude of which is consistent with downslope movements.

the instrumentation are described elsewhere (Matsuoka, submitted).

3. Monitoring soil movements

Soil movements were observed on a south-facing stone-banked lobe located at 3070 m ASL. A color line was painted horizontally at the middle part of lobe inclining at 21°. The deformation of the line (movement of surface debris) was traced with a KE camera throughout the year (Fig. 1A). The line was redrawn every summer with a different color (orange, blue or red). KE provided oblique images of the line daily at 8:00, 12:00 and 16:00 h from August 2007 to August 2012 (Fig. 2B).

Intensive movements occurred annually in two periods, from late September to middle November and from middle April to early June. The painted line was stable during the rest of the year. During the active periods the uppermost 5 cm of soil frequently experienced diurnal freeze-thaw cycles, most of which were accompanied by heave-settlement cycles recorded with an extensometer. Each frost heaving (needle ice or shallow ice lens) amounted to 0.5–2.0 cm (Fig. 2A) and frost heave (and thaw settlement) cycles occurred 40–70 times annually. These results indicate that diurnal frost creep dominates the slope movement on the lobe.

Stereographic vision of a pair of images at 8:00 (heaved) and at 12:00 or 16:00 (settled) displays three-dimensional frost heaving: the image is distorted according to a spatial variation in heave amounts. In fact, the stereogram showed that the central part of the lobe heaved more than the margins, which was consistent with a spatial variation in downslope movements (Fig. 2B).

Seasonal variation in the rate of frost creep is quantified by tracing the painted line on images at regular time intervals. The area enclosed by the deformed line and the datum gives the surface movement, which can be calibrated by a comparison with the area determined by an on-site measurement (Matsuoka, submitted).

In addition to frost creep, an episodic movement occurred once in the 2009–2010 period. Rapid soil movement removed a soil mass 80 cm wide and 20 cm thick; as a result, part of the painted line disappeared from view (Fig. 1). The time series images indicated that rill erosion occurred between 12:00 and 16:00 on 22 April 2010 (Fig. 3). Both images just before and after the erosion displayed rainy weather. In fact, a comparison with precipitation and soil temperature data suggested that (1) soil was frozen down to 60 cm or deeper during the previous night, (2) a heavy rainfall caused rapid thawing of the uppermost 10 cm of soil and (3) the supersaturated topsoil finally failed and flowed down (Fig. 4).

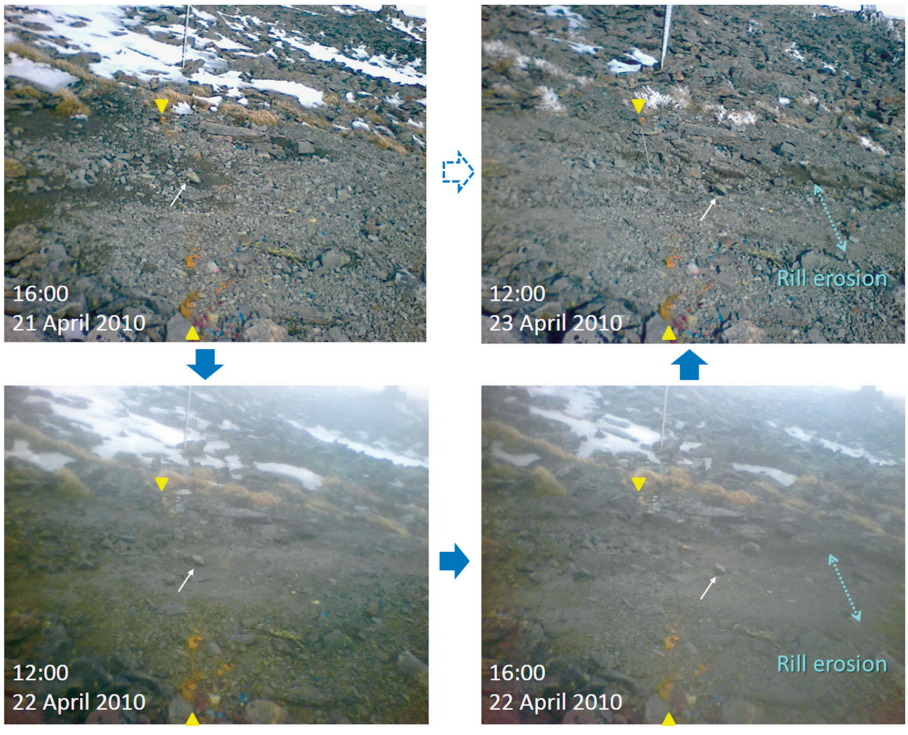

Fig. 3. Rill erosion generated between 12 h and 16 h on 22 April 2010. Left and right images display conditions before and after the rill erosion, respectively. The dark and foggy features of the lower images (note: the contrast is artificially enhanced) indicate rainy weather during rill erosion. The quarried zone (bidirectional arrow) and a displaced stone (small arrow) demonstrate rapid rill erosion. Yellow triangles represent the datum line.

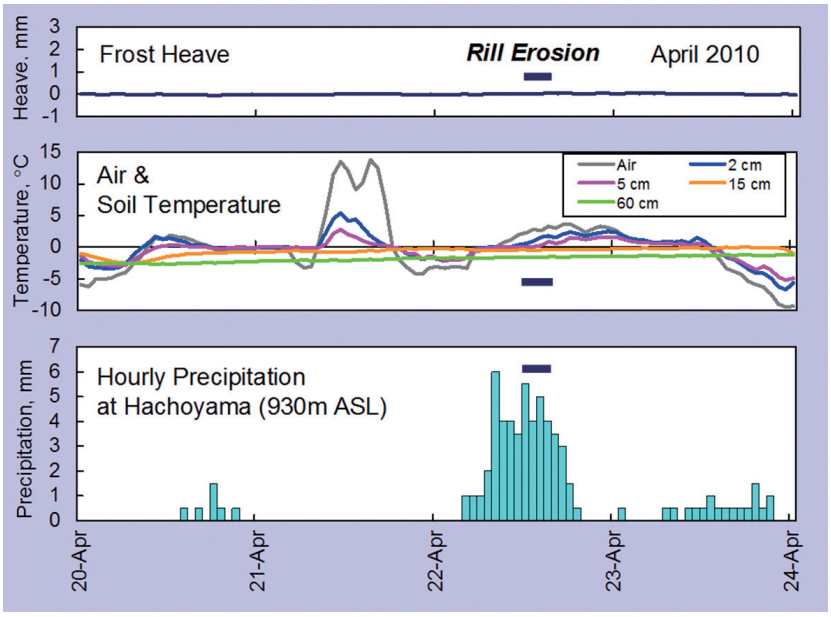

Fig. 4. Soil heave, temperature and precipitation during rill erosion. Rain data derive from the nearest public weather station (Hachoyama site), because on-site data were missing.

4. Monitoring rockfalls

Rockfalls were observed on the lower part of the Aresawa rockslide scarp, located in the southeastern slope of Mt. Ainodake, where various types and scales of rock failures are active (Nishii and Matsuoka, 2012). During the 1980s, small-scale rockfalls were investigated in terms of spalling from painted rock faces, but seasonal change in their activity was only roughly constrained (Matsuoka, 1990).

Interval cameras (KE and TLC) mounted on a pole have recorded images of the rockwall at a distance of 30–50 m since June 2011 (Fig. 5). KE provided images at 8:00, 12:00 and 16:00 h until September 2011 and thereafter daily images at 9:00 h. In addition, TLC have operated daily at 11:00 h since October 2012. The timing and magnitude of rockfalls were identified by examining the time series images. The year-round images also showed that the steep rockwall was largely snow-free throughout the winter, apart from temporary snow covers immediately after snowfalls and from snow-favored locations like couloirs.

Fracture of color-painted quadrangles (50×50 cm) indicated centimeter- to decimeter-scale rockfall events. In the 2012–2013 period, KE images were only available until 29 December, while TLC operated throughout the year despite having recorded red-filtered images between 12 November and 8 May. The TLC images showed significant spalling from the quadrangles (P3 and P4) during the winter (Fig. 6). Careful examination of red-filtered images revealed that most of the spalling occurred within two periods of mid-March (Fig. 6B), between 11th and 14th (E1) and between 16th and 17th (E2). Sensor-based monitoring indicated that these periods corresponded to the beginning of seasonal thawing, during which the rockwall experiences both diurnal freeze-thaw alternations within the outermost 20 cm and progressive warming of the still-frozen substrate (Fig, 7). Both rock temperatures and images indicated a temporary snow cover during the E1 event, which was a possible moisture source for rock joints. The subsequent diurnal freeze-thaw cycles may have promoted loosening of the rock joints and triggered the spalling events.

Stereographic view of successive images allowed identifi-

Fig. 5. Monitoring rockfalls from a rockslide scarp. The blue-painted quadrangles are 50×50 cm in area. KE = KADEC-EYE II camera. TLC = TimelapseCam 8.0 camera.

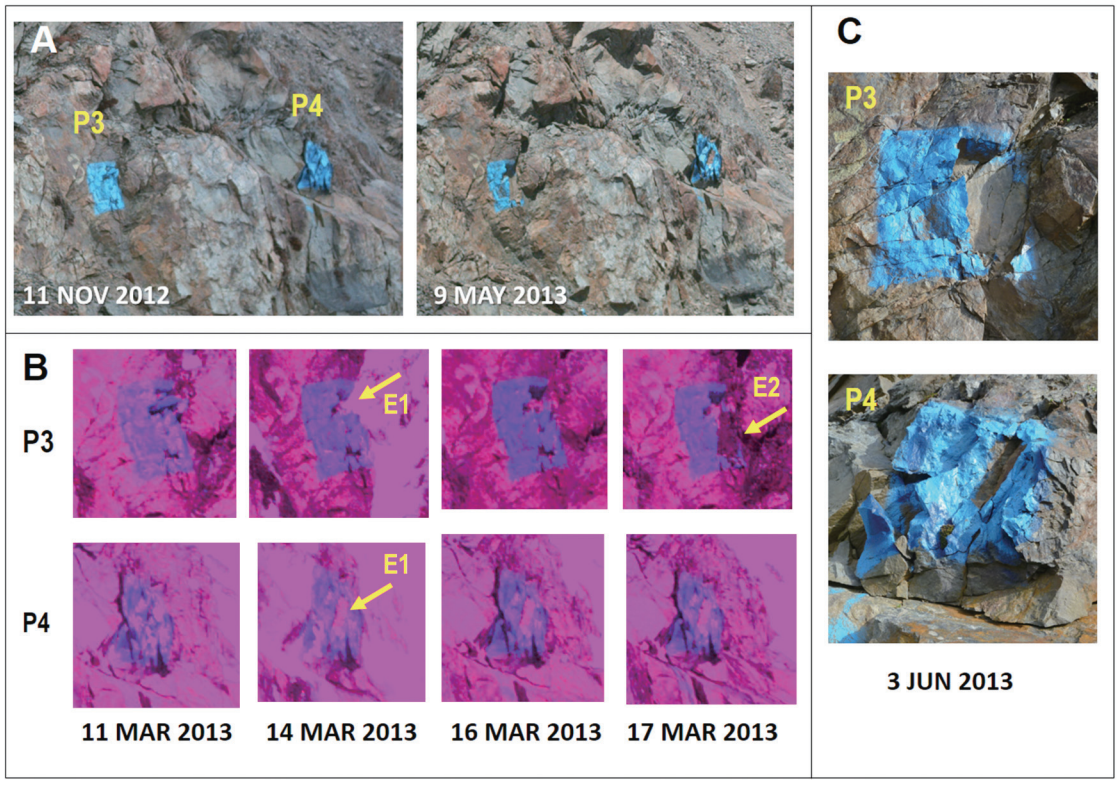

Fig. 6. Detachments from the quadrangles in March 2013. (A) TLC provided normal images of quadrangles (P3 and P4) only before 11 November 2012 and after 9 May 2013. (B) TLC produced red-filtered images between the two images in A, but the images included major spalling events (E1 and E2). (C) Close-up views of the quadrangles manually taken in June 2013.

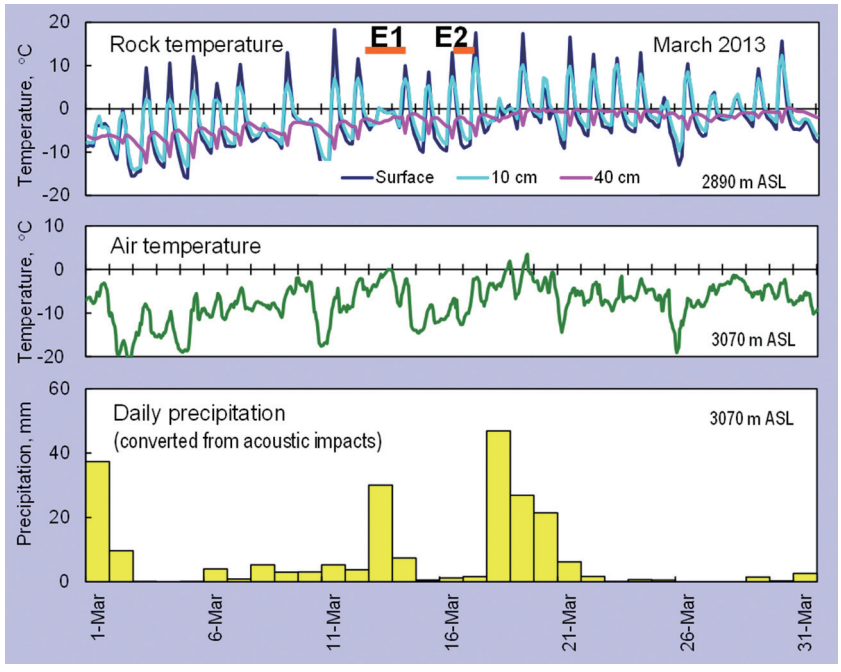

Fig. 7. Data from multisensor monitoring, showing the environmental conditions during the spalling events (E1 and E2) in March 2013. Note that the amount of precipitation is not accurate, since conversion from acoustic impacts assumed rainfalls, but most of the precipitation during this period is likely to have occurred as snowfalls.

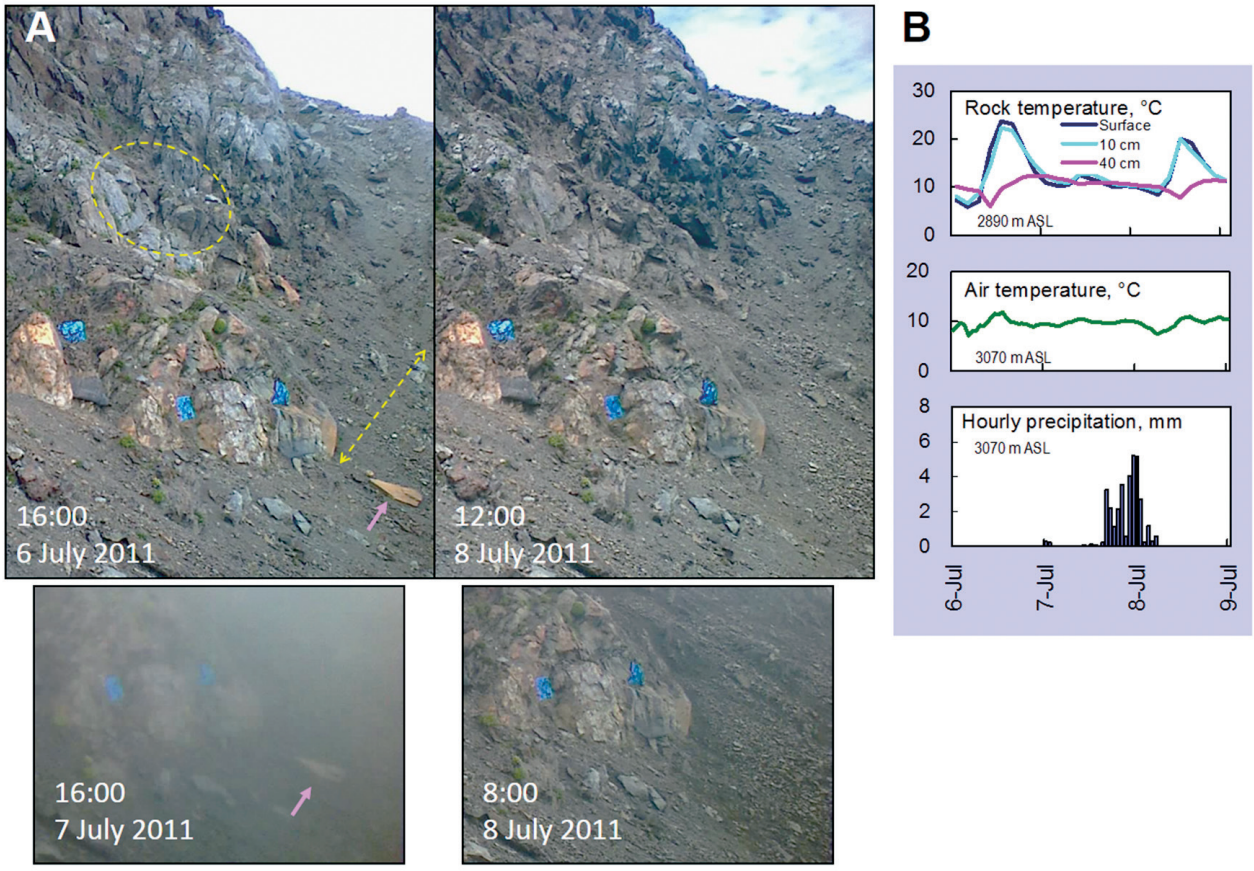

Fig. 8. A block fall in July 2011. (A) KE images before (left) and after (right) the block fall. The stereographic view of the upper pair displays the removal of blocks from the encircled rock face and a significant disturbance of the talus slope underneath (bidirectional arrow) including the disappearance of a platy stone (pink arrow). The block fall occurred between 16 h on 7 July and 8 h on 8 July as indicated the lower foggy images. (B) Meteorological and rock thermal conditions during the block fall.

cation of block-scale rockfalls, because any geomorphic change is seen as a disturbance. Such an event occurred between 16:00 h on 7 July and 8:00 h on 8 July 2011 (Fig. 8). A basal part of the rockfall collapsed and a subsequent debris avalanche removed the downslope talus materials. Meteorological data implied that nocturnal rainfall (total 33 mm) triggered this event.

5. Summary

Time-lapse photography greatly improves understanding of slope processes, having the following advantages:

(1) Time series images detect the timing of slope movements at a high temporal resolution.

(2) Stereographic view of successive images displays the location and magnitude of movement in a 3D image, which may be overlooked by sensor-based monitoring.

(3) When combined with sensor-based monitoring, time-lapse photography allows evaluation of thresholds (environmental controls) at which the movement occurs.

Acknowledgements

The field observations have been supported by the Grants-in-Aid for Scientific Research (17300294, 20300293, 23300334) from the Japan Society for the Promotion of Science and a special research promotion program entitled 'Program on Recovering Earth's Environments' from the Ministry of Education, Culture, Sports, Science and Technology in Japan. I wish to thank Tadashi Fukasawa, Ryoko Nishii and Atsushi Ikeda for their support of the fieldwork.

References

Barchyn, T.E. and Hugenholtz, C.H. (2012): Winter variability of aeolian sediment transport threshold on a cold-climate dune. *Geomorphology,* **177–178**, 38–50.

Christiansen, H.H. (2005): Thermal regime of ice-wedge cracking in Adventdalen, Svalbard. *Permafrost Periglac. Process.,* **16**, 87–98.

Girard, L., Gruber, S., Weber, S. and Beutel, J. (2013): Environmental controls of frost cracking revealed through in situ acoustic emission measurements in steep bedrock. *Geophys. Res. Lett.*, **40**, 1748–1753.

Harris, C., Kern-Luetschg, M., Christiansen, H.H. and Smith, F. (2011): The role of interannual climate vari-

ability in controlling solifluction processes, Endalen, Svalbard. *Permafrost Periglac. Process.,* **22**, 239–253.

Matsuoka, N. (1990): The rate of bedrock weathering by frost action: field measurements and a predictive model. *Earth Surf. Process. Landforms,* **15**, 73-90.

Matsuoka, N. (1998): Modelling frost creep rates in an alpine environment. *Permafrost Periglac. Process.,* **9**, 397–409.

Matsuoka, N. (2006): Monitoring periglacial processes: Towards construction of a global network. *Geomorphology*, **80**, 20–31.

Matsuoka, N. (submitted): Combining time-lapse photography and multisensor monitoring to understand frost creep dynamics in the Japanese Alps. *Permafrost Periglac. Process.*

Matsuoka, N. and Sakai, H. (1999): Rockfall activity from an alpine cliff during thawing periods. *Geomorphology*, **28**, 309-328.

Nishii, R. and Matsuoka, N. (2012): Kinematics of an alpine retrogressive rockslide in the Japanese Alps. *Earth Surf. Process. Landforms*, **37**, 1641-1650.

Scambos, T.A., Ross, R., Haran, T., Bauer, R., Ainley, D.G., Seo, K.-W., Keyser. M.De., Behar, A. and MacAyeal, D.R. (2013): A camera and multisensor automated station design for polar physical and biological systems monitoring: AMIGOS. *J. Glaciol.,* **214**, 303–314.

Received 11 September 2013
Accepted 21 October 2013